

PARTICULATES GENERATION AND SOLUTIONS FOR THEIR ELIMINATION IN PULSED LASER DEPOSITION

E. György^{*}, I. N. Mihailescu, M. Kompitsas^a, A. Giannoudakos^a

Lasers Department, Institute of Atomic Physics, P. O. Box MG 54, 077125 Bucharest, Romania

^aNational Hellenic Research Foundation, Theoretical and Physical Chemistry Institute, Vasileos Konstantinou Ave. 48, 11635 Athens, Greece

The presence of particulates of various shapes and dimensions on surfaces and incorporated into the bulk stands for the main drawback of pulsed laser deposited structures. The full understanding of the particulates generation mechanisms and development of techniques for their density reduction aiming to the complete elimination are key steps for future technological applications of laser deposited thin films. The choice of proper experimental conditions as the ablating laser wavelength and fluence, the target-collector separation distance, and the ambient gas pressure allows for the significant decrease of the particulates density, but not for the complete elimination. Several techniques have been proposed to reduce the particulates density. Nevertheless, the deposition of completely particulates free thin films was not yet reported. We used in our experiments a two synchronised pulsed laser system for the deposition of thin films and multistructures. The first, UV laser pulse ($\lambda=193$ nm, $\tau_{FWHM}\sim 10$ ns) is applied to ablate the target material and the second IR laser pulse ($\lambda= 1.064$ μm , $\tau_{FWHM}\sim 10$ ns) is directed parallel with the target surface. The role of second IR laser pulse is to heat and vaporise the particulates present in the tail of the ablation plasma generated by the first UV laser pulse. By optimising the time-delay between the two laser pulses we succeeded to deposit structures completely-free of particulates.

(Received July 9, 2003; accepted after revision January 28, 2004)

Keywords: Pulsed laser irradiation, Thin films deposition, Particulates, Synchronised laser systems

1. Introduction

Pulsed Laser Deposition (PLD) and Reactive PLD (RPLD) are important thin films synthesis techniques because they make possible the deposition of practically any kind of material with a rather simple experimental set-up. Some other advantages are the possibility to control film thickness and stoichiometry, the extreme purity of deposited material, as well as the growth of crystalline film at relatively low substrate temperature [1-6]. Nevertheless, the major drawback of thin films obtained by PLD/RPLD was related to the presence of micrometer and sub-micrometer sized particulates on films surface or embedded into their bulk. These particulates hamper the implementation of pulsed laser deposited structures in key technological fields, where completely particulate-free surfaces are required.

The main issues which contribute to particulates formation are the morphology of the target surface, target density, laser wavelength and fluence, ambient gas nature and pressure, and/or the target-collector separation distance. According to literature, the physical processes which lead to particulates formation are: (i) explosive dislocation of the substance caused by subsurface overboiling of target, (ii) gas phase condensation (clustering) of the vaporised material, (iii) liquid phase expulsion under recoil pressure of ablated substance, (iv) blast-wave explosion at liquid (melt) – solid interface and/or (v) hydrodynamic instabilities evolving on target surface [1-8].

^{*} Corresponding author: eniko@ifin.nipne.ro

The optimisation of process parameters (use of smooth target surface, combined rotation and scanning the target with respect to the laser beam, proper choice of distance target-collector surface, tilting of substrate orientation against the direction of the plasma-plume expansion, off-axis deposition, appropriate choice of the laser wavelength and fluence, as well as ambient gas nature and pressure) led to the reduction of the particulates density [9-12]. Besides, several other techniques have been developed to decrease the density of particulates, if possible till their complete exemption. These are mainly shadow masks, magnetic filters, gas jet directed into the plume during film growth, post-deposition annealing, or dual-laser beam ablation from one target [13-17]. A significant reduction of particulates was noticed, but not a complete elimination was obtained. One special mention is related to the fragmentation of particulates by means of an additional laser beam propagating parallel to target surface. It was demonstrated that this technique allows for the reduction of particulates density [18-20]. Nevertheless, the particulates complete elimination was not reached, possibly because of the improper choice of the delay time between ablating and reheating laser pulses.

We previously investigated the particulates formation mechanisms, as well as their structure and composition for various target material-ambient gas systems [21-26]. Our experimental evidences show that particulates generation mechanisms depend on physical properties of the target and processing parameters (e.g. laser wavelength, duration and fluence, as well as ambient gas nature and pressure). In recent experiments we used two synchronised laser sources for deposition of thin films [27,28].

The objective of these experiments was the reduction of particulates density aiming to the deposition of particulate-free thin films and multistructures. Our innovation was to combine an UV laser for target ablation with a second IR laser for plasma heating and particulates elimination. The first UV laser pulse was focused on the target surface to generate the ablation plasma. The second IR one was directed parallel to surface. The distance from target where the IR beam intercepted the ablation plasma was optimised after numerical simulations and experimental investigations. We demonstrated that the positive role of the second laser pulse is to heat and evaporate the particulates present in the tail of ablation plasma, during its transit from target to collector surface.

We report herewith an extended theoretical background, a review of previous results, along with the presentation of new experimental data.

2. Experimental

The experimental set-up is presented schematically in Fig. 1. The irradiations were performed inside a stainless steel vacuum chamber evacuated down to a residual pressure of 7×10^{-4} Pa prior to each deposition cycle. For Ta ablation we applied pulses generated by an ArF* excimer laser, ($\lambda=193$ nm, $\tau_{FWHM} \sim 10$ ns) at 10 Hz repetition rate. The laser beam incidence angle was of $\sim 45^\circ$.

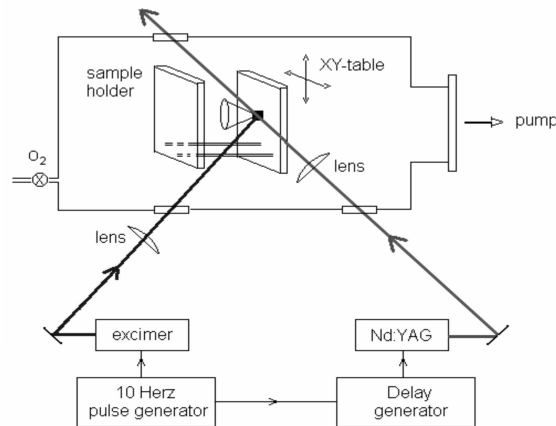


Fig. 1. Experimental set-up.

The IR pulses were generated by a controllable, time-delayed Nd:YAG ($\lambda = 1.064 \mu\text{m}$, $\tau_{\text{FWHM}} \sim 10 \text{ ns}$) laser. Pulses have been directed parallel to the target surface. The laser beam was crossing the flux of the ablated substance at a distance of 2 mm above ablation area. A FL 10 cm cylindrical lens focused the laser beam on the plane containing symmetry axis of the UV laser generated ablation plasma.

The controlled delay between the UV and IR laser pulses was set with a stable and high precision digital delay generator. The two laser pulses were recorded with a fast photodiode (rise time $< 1 \text{ ns}$) and monitored on a 350 MHz oscilloscope. The time jitter between the laser trigger and light pulses generated by the two laser systems was of a few ns only. Consequently, the delay time of interest in our experiments, from 10 μs to 1 ms, could be measured with a relative accuracy of $5 \times 10^{-2} - 5 \times 10^{-4}$. We point out that no long term drift was detected during the deposition time.

The ArF* laser fluence incident on target was of 0.75 J/cm². For the deposition of one film, we applied 50000 subsequent laser pulses. The IR laser pulse energy was varied from 50 to 250 mJ, which corresponds to a fluence of approximately (2.5-12) J/cm².

The ablated substance was deposited on glass slides placed plan-parallel with the target surface and kept at room temperature. The target - collector separation distance was 35 mm. To avoid fast drilling, the targets were mounted on a vacuum-compatible XY translator. This was computer controlled and performed a meander-like movement, both vertically and horizontally. We scanned a square surface of 10 \times 10 mm². The movement was selected that every target point inside the ablated area was irradiated by 5 laser shots before the translator is shifted to the next point 0.5 mm apart. The substrate holder was also connected to the XY translator, performing an identical movement as that of target. This movement synchronisation essentially contributes to the improvement of deposited film uniformity.

The morphology of deposited structures was investigated by scanning electron microscopy (SEM) with Cambridge S120 or JEOL TEMSCAN 200CX instruments.

3. Results and discussion

3.1. Theoretical considerations versus experimental results

3.1.1. Particulates formation by explosive dislocation of the substance caused by the subsurface overboiling of the target

We can evaluate the temperature distribution profile in the target bulk under the action of the laser pulse, at a distance ζ from the surface. To this purpose, the heat losses should be considered at the surface due to vaporisation [3]:

$$\Theta(\zeta) = \frac{I_0 A}{c\rho[v_{\text{vs}} - \alpha D_T]} \exp[-\alpha\zeta] - \frac{1}{2c} \left\{ H_v + \frac{I_0 A}{c\rho^2 v_{\text{vs}} - \alpha D_T} \right\} \exp\left[-\frac{v_{\text{vs}}\zeta}{D_T}\right] \quad (1)$$

In Eq. (1) I_0 stands for the laser pulse intensity, A target absorptivity, c specific heat, ρ mass density, α optical absorption coefficient, D_T heat diffusivity, H_v target vaporisation enthalpy, and v_{vs} velocity of vapor-solid interface.

According to our numerical simulations, the maximum temperature is reached in case of Ti at 30 nm beneath the target surface. Oppositely, this maximum is preserved on the surface in the case of Al targets. These results are generally congruent with calculations of A. Miotello and R. Kelly [29] which predicted that the effect of sub-surface overheating is not significant in case of good heat conductive targets, as Al. On the other hand, the sub-surface overheating effect is determined by a competition between volume heating, surface cooling due to vaporisation and heat dissipation into the target bulk. Numerical estimations of the balance between these processes have revealed the existence of considerable sub-surface heating in case of dielectric or poor conductive metal targets, even at low laser fluences [30].

3.1.2. Gas phase condensation (clustering) of the ablated material

Recent investigations have shown that the size of particulates formed by gas phase condensation of ablated species can be controlled by the molecular weight and pressure of the ambient gas, and/or target-collector separation distance [31,32]. Concretely, the density of particulates depends on the ambient gas nature, increasing with molecular gas weight. Also, the structure and size of clusters depend on the ablating laser fluence and pulse duration. Clustering is determined also by secondary processes occurring on films surface such as coalescence and enhanced mobility. These last two processes play a key role during deposition of relatively hot clusters [33].

We found that both particulates size and density are influenced by the presence of a gas inside the deposition chamber [28]. As compared to depositions in vacuum, the particulates observed in case of an ambient gas are larger but their density is lower. Indeed, the presence of ambient gas favours both the clustering and coalescence of small particulates. The increase of the particulates size with increase of the ambient oxygen pressure was reported also by Hino et al. [34] for KrF* excimer laser ablation of Ta targets.

3.1.3. Liquid phase expulsion under the action of the recoil pressure of the ablated substance

The total momentum imparted over the entire molten area, during the action of laser pulse results from [2]:

$$\iiint P_1 dx dy dt \approx P_1 \pi X_0^2 \tau \quad (2)$$

Here, P_1 stands for the pressure at the vaporisation front, $P_1 - P_s(T_s)$, $P_s(T_s)$ saturated vapor pressure at T_s - surface temperature, X_0 is the laser spot dimension incident on the target surface and τ the duration of the laser pulse.

We performed numerical simulations of the vapor pressure at the upper border of the Knudsen layer (which represents the distance from the vaporisation front where the ablated material reaches an equilibrium velocity distribution). We also estimated the pressure exerted by the vapor backward to the liquid (melt) substance in case of XeCl* excimer laser irradiation of Ti in 50 Pa nitrogen. The vapor flux has a maximum value of approximately 10 Kg/cm²s, i.e. a few µg during the action of every laser pulse. Thus, using equation (2), we inferred a value of $M_r \cong 0.4$ dyn.s. Such a momentum could prove strong enough to spray the liquid in form of a droplets jet [35,36].

The different composition of small and large particulates on the surface of TiC thin films obtained by RPLD from Ti in low-pressure CH₄ support their expulsion in liquid phase directly from the melt inside the crater under the recoil of plasma and vapors pressure [25]. The small particulates, generally spherical, consist of TiC only. The larger ones include an important amount of un-reacted Ti besides a certain quantity of TiC. We assume that the carbon content inside the molten surface layer presents a high gradient with a superficial strong contamination with carbon above a deep content of bare melted Ti. Accordingly, under the vapour and plasma recoil pressure, liquid droplets are sprayed out from melted pool, with different chemical composition.

Our recent investigations revealed that the increase of ablating UV laser fluence leads to the increase of the particulates size and density on the deposited films surfaces [27]. Thus, the ablation fluence was reduced down to 0.75 J/cm², a value slightly exceeding the reported evaporation threshold of Ta. Indeed, the deposited film was much smoother, with reduced particulates presence (Fig. 2). The spherical shape of particulates and their size within the sub-micrometer and micrometer range indicate that most probably they were expelled in liquid phase, under the expanding ablated substance (vapour and plasma) recoil pressure.

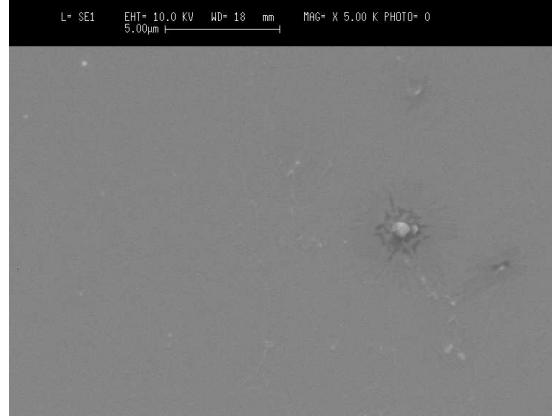


Fig. 2. SEM image of a thin film deposited by ArF* ($\lambda=193$ nm, $\tau_{FWHM}\sim 10$ ns) laser irradiation with a fluence of 0.75 J/cm² in vacuum. The mark corresponds to 5 μ m.

3.1.4. Blast-wave explosion at the liquid (melt) – solid border

Under certain conditions, a fraction of the incident laser beam, which crosses the plasma, can penetrate down to the liquid (melt) – solid interface. There it can ignite a punctual blast wave explosion. The blast pressure in liquid at the solid metal – liquid interface, caused by liquid breakdown, was inferred under the hypothesis of a point-like explosion [37]:

$$P \approx \left[\frac{\gamma - 1}{\pi} \right]^{2/5} \left(\frac{\rho_l^3 E_p^{1/5}}{\tau^6} \right)^{1/5} \quad (3)$$

In Eq. (3) ρ_l stands for the density of the liquid state, γ is the adiabatic index of the breakdown plasma in liquid, E_p is the laser energy absorbed by the plasma, and τ is the laser pulse duration. We assume $E_p < E_0$, the laser pulse energy. If we suppose that $E_p \approx 0.1 \times E_0$, this pressure can reach a few hundreds of MPa. This pressure is sufficient not only to expel liquid droplets, but also to dislocate frozen neighbouring solid fragments. They are deposited on film in form of polyhedral particulates [24].

3.1.5. Hydrodynamic instabilities

Different types of hydrodynamic instabilities have been suggested, which could promote growth of large scale periodic surface structures (in form of quite high amplitude waves), and ejection of micrometer sized liquid droplets. According to Refs. 3, 7, and 8 particulates generation from molten layers and their subsequent expulsion could be due to Kelvin-Helmholz and Rayleigh-Taylor instabilities in the presence of laser induced plasma. Alternative mechanisms are capillary waves caused by variations of the surface tension in connection to local surface temperature. We note that under our irradiation conditions as described in Ref. 26, capillary waves could produce a surface microrelief with a periodicity of a few tens of micrometers. This prediction was found in good agreement with the results of SEM investigations of Si targets submitted to multi-pulse laser irradiation in low-pressure ammonia [26]. The periodicity of droplets within the crater is indicative of hydrodynamic instabilities evolving along the target surface.

3.2. Deposition of particulate-free thin films by a system with two synchronised laser sources

We used a second IR laser directed parallel with the target surface with the purpose to intercept, heat and break the particulates present in the ablation plasma plume (see Fig. 1). The choice

for a second pulsed laser source in IR is due the higher absorption at these wavelengths by vapors, plasma and particulates. This is mainly driven by the inverse Bremsstrahlung (IB) process in the initial plasma [2,3]. Indeed, the characteristic absorption coefficient is proportional to the square of the incident laser wavelength. Correspondingly, this effect is minor for wavelengths in UV. Moreover, due to the supplementary kinetic energy gained from radiation by IB, free electrons excite and ionise the vapour species by electron collisions [4]. Accordingly, the second IR laser pulse plays a double role: direct heating, breaking, and evaporation of particulates present in the ablation plasma, and increasing kinetic energies of the plume species. This last effect directly contributes to the particulates evaporation in the ablation plasma. Also, a higher degree of excitation of species, allowing for enhanced gas phase reactions and ensures better films adhesion, crystallinity and morphology [1-3].

As known, the sub-micrometer and micrometer size particulates travel with the “tail” of the laser ablation plasma [3,37]. They have propagation velocities of 10^3 cm/s to 10^4 cm/s, about two orders of magnitude lower than atomic and molecular species [38]. The time delay between UV and IR laser pulses was accordingly adjusted at 200 μ s. The obtained thin film surface was smooth, and free of particulates (Fig. 3). This observation is fully supporting our ideas that the IR pulses effectively intercepted the “tail” of UV plasma plume containing particulates travelling with an average velocity of 10^3 cm/s. For larger delay times than the optimum value we observed the re-appearance of particulates on the surface of deposited films.



Fig. 3. SEM image of a thin film deposited in vacuum by the two synchronised lasers system. The UV and IR laser fluences were 0.75 J/cm² and 8 J/cm², respectively. The time delay between the UV and IR laser pulses was 200 μ s. The mark corresponds to 5 μ m. The complete elimination of particulates is evident.

4. Conclusions

The particulates formation mechanisms in PLD/RPLD are determined by the specific optical and thermo-physical properties of the target, as well as irradiation conditions. The use of lower values for incident UV laser fluence results in the decrease of particulates density. This decrease can be the effect of a lower recoil pressure of the laser generated ablation plasma. Another important parameter which influences the particulates formation and size is the ambient gas nature and pressure. We found that with the increase of gas pressure, density of particulates decreases, but their size increases due – the most probably- to enhanced number of collisions of the ablated species along with coalescence of small particulates.

We developed a system with two synchronised laser sources to diminish the particulates density until their complete exemption. Our choice was made for 2 laser sources generating ns pulses in UV and IR respectively. Our reasons were that UV laser pulses couple very well with solid and liquid targets, while IR laser pulses are more efficiently absorbed by vapors and plasma. The second IR laser was directed perpendicularly to the UV laser generated ablation plasma to intercept, heat and

break the particulates during their transit from target to collector. As expected, the IR laser pulses efficiently couple with the “tail” of ablated plasma containing vapors, ionic species and especially particulates. This slow tail travels with an average velocity of 10^3 cm/s – i.e. about 2 orders of magnitude lower than the leading plasma front, which does not contain particulates.

By the proper choice of the processing parameters, as well as time delay values between the ablating UV and the second IR laser pulses, we succeeded to reduce the particulates density, until their complete elimination.

A last mention is that these results also evidence a small contribution, if any, of clustering mechanism in particulates formation. Indeed, this mechanism should be active throughout plasma length during its expansion from target to collector. In other words, it would have been impossible to eliminate particulates by interception of the plasma “tail” only, if clustering mechanism would have remained active during all plasma expansion.

Acknowledgements

The authors acknowledge with thanks the financial support of a NATO PST.CLG.977325 Collaborative Linkage Grant and additional financing from a Greek-Romanian Joint Research and Technology program on “Multiwavelength laser plasma investigations for applications in thin films deposition and processing”.

References

- [1] D. B. Chrisey, G. K. Hubler (eds), “Pulsed Laser Deposition of Thin Films”, Wiley, New York, 1994
- [2] M. Von Allmen, A. Blatter, “Laser-Beam Interactions with Materials”, 2nd edn., Springer, Berlin, 1995
- [3] D. Bauerle, “Laser Processing and Chemistry”, 2nd edn., Springer, Berlin, 1996.
- [4] W. W. Duley, “UV Lasers: effects and applications in materials science”, University Press, Cambridge, 1996.
- [5] I. N. Mihailescu, E. Gyorgy, “Pulsed Laser Deposition: An Overview”, Invited contribution to the 4-th International Commission for Optics (ICO) Book "Trends in Optics and Photonics", ed. T. Asakura (ICO President) Springer Series in Optical Science, pp. 201, 1999.
- [6] K. Murakami, in “Laser Ablation of Electronic Materials – Basic Mechanisms and Applications”, ed. By E. Fogarassy, S. Lazare, Elsevier, Amsterdam, 125, 1992.
- [7] R. Kelly, J. Rothenberg, Nucl. Instrum. Methods B **7/8**, 755 (1985).
- [8] A. B. Brailovsky, S. V. Gaponov, V. I. Luchin, Appl. Phys. A **61**, 81 (1995).
- [9] E. Agostinelli, S. Kaciulis, M. Vittori-Antisari, Appl. Phys. Sci. **156**, 143 (2000).
- [10] N. Inoue, S. Kashiwabara, S. Toshima, R. Fujimoto, Appl. Surf. Sci. **96-98**, 656 (1996).
- [11] Y. Watanabe, M. Tanamura, S. Matsumoto, Y. Seki, J. Appl. Phys. **78**, 2029 (1995).
- [12] T. E. Itina, A. A. Katassonov, W. Marine, M. Autric, J. Appl. Phys. **83**, 6050 (1998).
- [13] D. Lubben, S. A. Barnett, K. Suzuki, S. Gorbalkin, J. E. Greene, J. Vac. Sci. Techn. B **3**, 968 (1985).
- [14] S. J. Barrington, T. Bhutta, D. P. Shepherd, R. W. Eason, Optics Communication **185**, 145 (2000).
- [15] R. Jordan, D. Cole, J. G. Lunney, Appl. Surf. Sci. **109-110**, 403 (1997).
- [16] R. Dat, O. Auciello, D. J. Lichtenwalner, A. I. Kingon, J. Mater. Res. **11**, 1514 (1996).
- [17] P. Mukherjee, S. Chen, J. B. Cuff, P. Sakthivel, S. Witanachchi, J. Appl. Phys. **91**, 1828 (2002).
- [18] G. Koren, R. J. Baseman, A. Gupta, M. I. Lutwyche, R. B. Laibowitz, Appl. Phys. Lett. **56**, 2144 (1990).
- [19] H. Chiba, K. Murakami, O. Eryu, K. Shihoyama, T. Mochizuki, K. Masuda, Jpn. J. Appl. Phys. **30**, L 732 (1991).
- [20] C. H. Becker, J. B. Pallix, J. Appl. Phys. **64**, 5152 (1988).

- [21] V. S. Teodorescu, I. N. Mihailescu, E. Gyorgy, A. Luches, M. Martino, L. C. Nistor, J. Van Landuyt, J. Hermann, *J. Mod. Opt.* **43**, 1773 (1996).
- [22] I. N. Mihailescu, Lita, V. S. Teodorescu, E. Gyorgy, R. Alexandrescu, A. Luches, M. Martino, A. Barborica, *J. Vac. Sci. Technol. A*, **14**, 1986 (1996).
- [23] G. Leggieri, A. Luches, M. Martino, A. Perrone, R. Alexandrescu, A. Barborica, E. Gyorgy, I. N. Mihailescu, G. Majni, P. Mengucci, *Appl. Surf. Sci.* **96**, 866 (1996).
- [24] N. Chitica, E. Gyorgy, A. Lita, G. Marin, I. N. Mihailescu, D. Pantelica, M. Petrascu, A. Hatzia Apostolou, C. Grivas, N. Broll, A. Cornet, C. Mirica, A. Andrei, *Thin Solid Films*, **301**, 71 (1997).
- [25] I. N. Mihailescu, V. S. Teodorescu, E. Gyorgy, A. Luches, A. Perrone, M. Martino, *J. Phys. D: Appl. Phys.* **31**, 2236 (1998).
- [26] I. N. Mihailescu, E. Gyorgy, V. S. Teodorescu, Gy. Steinbrecher, J. Neamtu, A. Perrone, A. Luches, *J. Appl. Phys.* **86**, 7123 (1999).
- [27] E. Gyorgy, I. N. Mihailescu, M. Kompitsas, A. Giannoudakos, *Appl. Surf. Sci.* **195**, 270 (2002).
- [28] E. Gyorgy, I. N. Mihailescu, M. Kompitsas, A. Giannoudakos, *Thin Solid Films*, **446** (2), 178 (2004).
- [29] A. Miotello, R. Kelly, *Appl. Phys. Lett.* **67**, 3535 (1995).
- [30] N. M. Bulgakova, A. V. Bulgakov, *Appl. Phys. A. Mater. Sci. Process.* **73**, 199 (2001).
- [31] D. H. Lowndes, C. M. Rouleau, T. G. Thundat, E. A. Kenik, S. J. Pennycook, *J. Mater. Res.* **14**, 359 (1999).
- [32] M. Inada, I. Umezumi, A. Sugimura, *J. Vac. Sci. Technol. A* **21**, 84 (2003).
- [33] W. Marine, L. Patrone, B. Luk'yanchuk, M. Sentis, *Appl. Surf. Sci.* **154-155**, 345 (2000).
- [34] T. Hino, M. Nishida, T. Araki, *Surf. Coat. Technol.* **149**, 1 (2002).
- [35] M. Von Allmen, *J. Appl. Phys.* **47**, 5460 (1976).
- [36] J. Neamtu, I. N. Mihailescu, C. Ristoscu, J. Herman, *J. Appl. Phys.* **86** (1999) 6096
- [37] R. T. Aratyunyan, V. Yu. Baranov, L. A. Bolshov, D. D. Mal'yuta, A. Yu. Sebrant, "Laser Beam Effects on Materials", Nauka, Moscow, 1989 (in Russian).
- [39] B. Hopp, N. Kresz, Cs. Vass, Z. Toth, T. Smausz, F. Ignacz, *Appl. Surf. Sci.* **186**, 298 (2002).